A Convenient gHMQC-Based NMR Assay for Investigating Ammonia Channeling in Glutamine-Dependent Amidotransferases: Studies of *Escherichia coli* Asparagine Synthetase B†

Kai K. Li, William T. Beeson, IV,‡ Ion Ghiviriga, and Nigel G. J. Richards*

Department of Chemistry, University of Florida, Gainesville, Florida 32611-7200

Received January 24, 2007

ABSTRACT: X-ray crystal structures of glutamine-dependent amidotransferases in their "active" conformation have revealed the existence of multiple active sites linked by solvent inaccessible intramolecular channels, giving rise to the widely accepted view that ammonia released in a glutaminase site is channeled efficiently into a separate synthetase site where it undergoes further reaction. We now report a very convenient isotope-edited ^{1}H NMR-based assay that can be used to probe the transfer of ammonia between the active sites of amidotransferases and demonstrate its use in studies of *Escherichia coli* asparagine synthetase B (AS-B). Our NMR results suggest that (i) high glutamine concentrations do not suppress ammonia-dependent asparagine formation in this bacterial asparagine synthetase and (ii) ammonia in bulk solution can react with the thioester intermediate formed during the glutaminase half-reaction by accessing the N-terminal active site of AS-B during catalytic turnover. These observations are consistent with a model in which exogenous ammonia can access the intramolecular tunnel in AS-B during glutamine-dependent asparagine synthesis, in contrast to expectations based on studies of class I amidotransferases.

Glutamine-dependent amidotransferases catalyze the release of ammonia from the side chain amide of glutamine and its subsequent transfer to a variety of electrophilic acceptors (*1*−*3*). X-ray crystal structures of these enzymes in their "active" conformation reveal the existence of multiple active sites that are linked by solvent inaccessible intramolecular channels (*4*−*13*). These structural observations have therefore given rise to the hypothesis that ammonia released in a glutaminase site is channeled efficiently into a second active site where it undergoes reaction with the appropriate nitrogen acceptor to complete the overall enzymatic transformation (*1*, *14*−*18*). On the other hand, kinetic evidence that supports this proposal has been obtained for relatively few glutamine-dependent amidotransferases (*19*−*22*). Perhaps the most convincing evidence for intramolecular ammonia channeling has come from ^{15}N NMR studies of carbamoyl phosphate synthetase (CPS)[1] (*19*, *23*−*25*), which demonstrated that $^{14}NH_3$ produced in the glutamine domain of CPS does not exchange with $^{15}NH_3$ present in bulk solution (*19*). In addition, pre-steady state kinetic measurements have shown the rates of ammonia utilization and glutaminase activity in CPS to be coupled, implying that only a single ammonia molecule is present in the intramolecular tunnel of the enzyme during catalytic turnover (*23*). Integrated structural, computational, and experimental measurements have also provided support for active site coupling and intramolecular ammonia transfer in imidazole glycerol phosphate synthase (IGPS) (*20*, *26*−*29*). Both CPS and IGPS are class I amidotransferases (*1*, *30*), however, and their molecular behavior may not therefore be representative of the evolutionarily unrelated class II (*1*, *31*) or class III amidotransferases (*32*).

Glutamine-dependent asparagine synthetase (ASNS) is a class II amidotransferase (*1*), which catalyzes the ATP-dependent formation of asparagine from aspartate using glutamine as the likely physiological nitrogen source (Scheme 1) (*15*, *33*). Both the mammalian and bacterial forms of the enzyme can accept free ammonia as an alternate substrate in vitro (*34*, *35*), and in sharp contrast to the behavior of other class II amidotransferases for which the independent catalytic sites are tightly coupled (*36*−*38*), the glutaminase and synthetase activities of ASNS appear to be only weakly coordinated even at saturating concentrations of L-glutamine, ATP, and L-aspartate (*39*−*41*). As a result, L-glutamate and L-asparagine are not formed in a 1:1 stoichiometry by either human ASNS (*39*) or the cognate enzyme in *Escherichia coli* (AS-B) (*40*, *41*) under steady state conditions unless glutamine is present at a very low concentration. This lack of active site coupling in ASNS is surprising in light of observations with other amidotransferases and raises ques-

† This work was supported by the Chiles Endowment Biomedical Research Program of the Florida Department of Health and the provision of an award from the University of Florida Undergraduate Scholars Program (W.T.B.).

* To whom correspondence should be addressed: Telephone: 352-392-3601. Fax: 352-846-2095. E-mail: richards@qtp.ufl.edu.

‡ Present address: Department of Chemistry, University of California, Berkeley, CA 94720.

[1] Abbreviations: NMR, nuclear magnetic resonance; CPS, carbamoyl phosphate synthetase; IGPS, imidazole glycerol phosphate synthase; ASNS, glutamine-dependent asparagine synthetase; AS-B, *Escherichia coli* glutamine-dependent asparagine synthetase; HEPPS, 3-[4-(2-hydroxyethyl)-1-piperazinyl]propanesulfonic acid; DMSO, dimethyl sulfoxide; DSS, sodium 2,2-dimethyl-2-silapentane-5-sulfonate; TCA, trichloroacetic acid; gHMQC, gradient heteronuclear multiple-quantum coherence; MD, molecular dynamics; TE, thioester intermediate.

10.1021/bi700145t CCC: $37.00 © 2007 American Chemical Society
Published on Web 03/31/2007

Scheme 1: Reactions Catalyzed by *E. coli* AS-B[a]

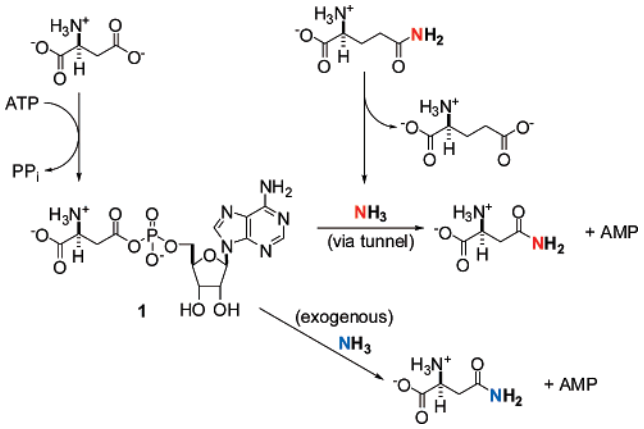

[a] The formation of β-aspartyl-AMP intermediate **1** and its reaction with ammonia both take place in the C-terminal synthetase site, while the hydrolysis of glutamine to yield enzyme-bound ammonia occurs in the N-terminal domain of the enzyme. In the competition experiments described herein, the amide nitrogen of asparagine comes either from glutamine via intramolecular channeling (red) or from $^{15}NH_3$ in bulk solution (blue).

tions about the structural integrity of the solvent inaccessible, intramolecular tunnel that is seen in the AS-B crystal structure (Figure 1) (*12*) as the enzyme proceeds through its catalytic cycle.

We now report the use of a very convenient isotope-edited ^{1}H NMR-based assay (*42*) that we have developed to probe the transfer of ammonia between the two active sites in AS-B. This gradient heteronuclear multiple-quantum coherence (gHMQC) method, which should be generally applicable for studies of other glutamine-dependent amidotransferases, has provided quantitative information about the extent to which ^{15}N is incorporated into the side chain of asparagine formed in the enzyme-catalyzed reaction. At least in the case of AS-B, the results of these gHMQC NMR studies show that (i) high glutamine concentrations do not suppress ammonia-dependent formation of asparagine by this enzyme and (ii) ammonia in bulk solution can undergo reaction with a thioester intermediate formed during the glutaminase half-reaction (*43*). These observations are consistent with a model in which exogenous ammonia can access the tunnel in AS-B during glutamine-dependent asparagine synthesis, in contrast to expectations based on studies of class I amidotransferases (*19*, *26*, *27*).

MATERIALS AND METHODS

Materials. Unless otherwise stated, all chemicals and reagents were purchased from Sigma (St. Louis, MO) and were of the highest available purity. [1,3-$^{15}N_2$]Uracil, [^{15}N]-L-asparagine, and d_6-DMSO were purchased from Sigma-Aldrich (St. Louis, MO). The level of isotopic incorporation in these samples was greater than 99%. All experiments employed freshly prepared solutions of recrystallized L-glutamine (*34*). Recombinant, wild-type AS-B was expressed and purified following literature procedures (*44*). Protein concentrations were determined using a modified Bradford assay (Pierce, Rockford, IL) (*45*), for which standard curves were constructed with bovine serum albumin, and corrected as previously reported (*36*). NMR spectra were recorded on a Varian INOVA 500 instrument equipped with a 5 mm triple-resonance indirect detection probe (*z*-axis gradients) operating at 500 and 50 MHz for ^{1}H and ^{15}N, respectively. Chemical shifts are reported in parts per million relative to sodium 2,2-dimethyl-2-silapentane-5-sulfonate (DSS). The coaxial inner cell (catalog no. NE-5-CIC-V) containing the external NMR standards was purchased from New Era Enterprises (Vineland, NJ).

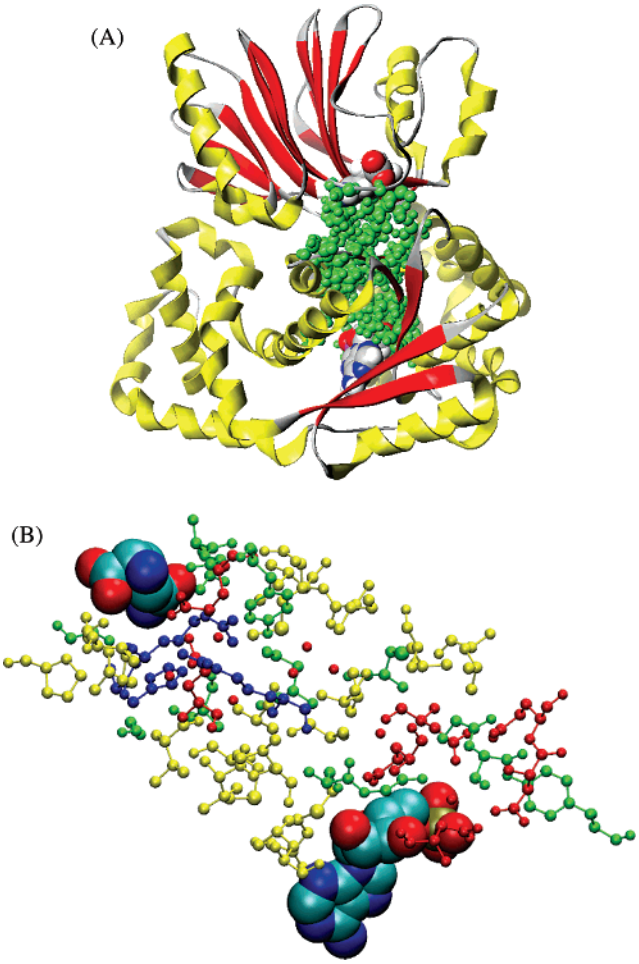

FIGURE 1: Cartoon representations of the *E. coli* AS-B monomer. (A) High-resolution X-ray structure of the enzyme (PDB entry 1CT9) (*12*) showing the structural elements that define the glutaminase and synthetase domains. In this cartoon representation, atoms in residues defining the tunnel connecting the active sites are rendered as green spheres, and α-helices and β-strands are colored yellow and red, respectively. Bound glutamine (top) and AMP (bottom) are shown as space-filling models in which hydrogen atoms bound to carbon atoms have been omitted for clarity. Atom coloring is as follows: C, black; H, white; N, blue; and O, red. (B) Close-up representation of the residues defining the ammonia tunnel, the body of which is formed primarily by hydrophobic residues (yellow). Acidic and polar (red) and basic (blue) residues are observed at the C-terminal and N-terminal ends of the tunnel, respectively. Residues with polar, uncharged side chains are also shown (green). Bound glutamine (top) and AMP (bottom) are again rendered as space-filling models, and red spheres represent crystallographic water molecules bound within the tunnel. These structures were visualized using the CAChe Worksystem Pro (Fujitsu America Inc., Beaverton, OR) and VMD (*56*) software packages.

NMR Measurements. Concentrations of [^{15}N]-L-asparagine were determined using a solution of [1,3-$^{15}N_2$]uracil dissolved in d_6-DMSO as a standard, which was placed in a coaxial inner cell inserted into the 5 mm tube containing the assay sample. The amount of [^{15}N]-L-asparagine was measured

using a phase-sensitive, one-dimensional gHMQC pulse sequence (*42*), as implemented in the Varian VNMR software package (version 6.1C). NMR spectra were acquired, at a fixed temperature of 25 °C, in 256 transients with a digital resolution of 0.25 Hz/point (25 966 points in the FID over a spectral window of 6492 Hz) using a relaxation delay of 1 s and an acquisition time of 2 s. The total time for acquiring each spectrum was therefore 13 min. The encoding gradient level was 37 G/cm with a duration of 2.5 ms, and the corresponding values for the decoding gradient were 18.7 G/cm and 1 ms, with a gradient recovery time of 0.5 ms. The 90° pulse times used in the experiment for ^{1}H and ^{15}N were 9.6 and 25.8 μs, respectively, and the $^{1}H-^{15}N$ coupling constant was set to a value of 87 Hz. The FID was weighted with a line broadening of 10 Hz and a Gaussian of 0.278 Hz.

Competition Experiments. Assay mixtures consisted of 60 mM $MgCl_2$, 10 mM ATP, 20 mM L-aspartic acid, and variable concentrations of $^{15}NH_4Cl$ and/or L-glutamine, dissolved in 100 mM HEPPS buffer (pH 8) (total volume of 2 mL). In experiments during which the concentration of L-glutamine was varied from 0 to 40 mM, the level of $^{15}NH_4Cl$ was fixed at an initial concentration of 100 mM. Alternatively, when the $^{15}NH_4Cl$ concentration was varied from 25 to 100 mM, L-glutamine was initially present at a concentration of 20 mM. Reactions were initiated by the addition of AS-B (31 μg) and the resulting samples incubated for 10 min at 37 °C before being quenched by the addition of trichloroacetic acid (TCA) (60 μL). After centrifugation for 5 min at 3000 rpm to remove precipitated protein, the supernatant was adjusted to pH 5 by the addition of 10 M aqueous NaOH and an aliquot of this solution (650 μL) transferred to a 5 mm NMR tube for analysis. At higher pH values, amide NH exchange precluded the derivation of any quantitative relationship between peak area and [^{15}N]Asn concentration.

^{15}N Exchange Experiments. Assay mixtures consisted of 60 mM $MgCl_2$, 10 mM ATP, and variable concentrations of $^{15}NH_4Cl$ and L-glutamine, dissolved in 100 mM HEPPS buffer (pH 8) (total volume of 2 mL). In experiments during which the concentration of L-glutamine was varied from 0 to 80 mM, the $^{15}NH_4Cl$ concentration was fixed at 100 mM. Alternatively, when the $^{15}NH_4Cl$ concentration was varied from 0 to 100 mM, L-glutamine was added at an initial concentration of 20 mM. As in the competition experiments, reaction was initiated by the addition of AS-B (62 μg), and the resulting samples were incubated for 10 min at 37 °C before being quenched with TCA (60 μL). After centrifugation for 5 min at 3000 rpm to remove precipitated protein, the supernatant was adjusted to pH 5 by the addition of 10 M aqueous NaOH and an aliquot of this solution (650 μL) transferred to a 5 mm NMR tube for analysis. At higher pH values, amide NH exchange precludes the derivation of any quantitative relationship between peak area and [^{15}N]Gln concentration.

HPLC-Based Determination of the Total Amount of L-Asparagine. To obtain an estimate of the total amount of L-asparagine in the final reaction mixtures, we employed a HPLC-based end point assay (*36*). Hence, an aliquot of each mixture (40 μL) was diluted (200 μL final volume) with 400 mM aqueous Na_2CO_3 (pH 9) containing 10% DMSO and 30% dinitrofluorobenzene (DNFB) (as a saturated solution in EtOH). The resulting solutions were heated at 50 °C for 45 min to permit reaction of DNFB with the amino acids to yield their dinitrophenyl (DNP) derivatives. **Caution**: Extreme care should be taken when handling solutions of 2,4-dinitrofluorobenzene in organic solvents because this reagent is a potent allergen and will penetrate many types of laboratory gloves (*46*). Aliquots of each assay mixture (20 μL) were analyzed by reverse-phase HPLC (RP-HPLC) using a C_{18} column and a flow rate of 0.7 mL/min. The DNP-derivatized amino acids were eluted using a step gradient of 40 mM formic acid buffer (pH 3.6) and CH_3CN. In this procedure, the initial concentration of the organic phase (CH_3CN) was 14%, which was maintained over a period of 26 min before the amount of CH_3CN was increased to 80% over a period of 30 s, and elution continued for a further 8 min. Eluted amino acid DNFB derivatives were monitored at 365 nm and identified by comparison to authentic standards. Under these conditions, DNP-asparagine exhibited a retention time of approximately 25 min and could be quantified on the basis of its peak area. Calibration curves were constructed using solutions of pure L-asparagine derivatized in the same manner as the samples.

Kinetic Simulations. Simulations were performed using the GEPASI software package (*47*, *48*).

RESULTS AND DISCUSSION

Competition Experiments. Two mechanisms can be envisaged for the transfer of nitrogen from the glutaminase to the synthetase active sites in AS-B. In the first, ammonia is directly transferred between the two active sites through an intramolecular tunnel (*4*−*13*). This proposal, which is hypothesized to occur in all other glutamine-dependent amidotransferases (*1*, *14*−*18*), is supported by X-ray crystallographic observations on the bacterial enzyme (*12*). A second model can be envisaged, however, in which ammonia is released into the bulk solution prior to re-entering the synthetase site and reacting with the β-aspartyl-AMP intermediate. We therefore sought a simple and rapid kinetic assay to distinguish between these possibilities, which might also be applicable in experiments aimed at developing structure−function relationships for residues defining the tunnel observed in AS-B. Early work on CTP synthetase (*49*−*51*) and GTP synthetase (*52*) aimed at investigating this problem employed the pH dependence of synthetase activity when glutamine and ammonia (or alternate substrates such as hydroxylamine) were both present in solution. We elected to employ an alternate, and somewhat more straightforward, strategy, however, in which the glutamine-dependent asparagine synthetase reaction was performed in the presence of exogenous $^{15}NH_4Cl$. In particular, we hoped to employ ^{15}N NMR spectroscopy to determine the extent of incorporation of ^{15}N into asparagine as a function of glutamine concentration, as previously reported in studies on CPS (*19*). The low sensitivity of the ^{15}N nucleus proved to be a significant limitation to our efforts, mandating a substantial investment of spectrometer time for obtaining spectra with sufficiently high signal-to-noise ratios for any quantitative measurements, thereby severely limiting the number of conditions under which competition studies could be carried out. We therefore investigated the use of a phase-sensitive one-dimensional gHMQC experiment (*42*) to measure the extent to which ^{15}N was incorporated into asparagine when AS-B was incubated

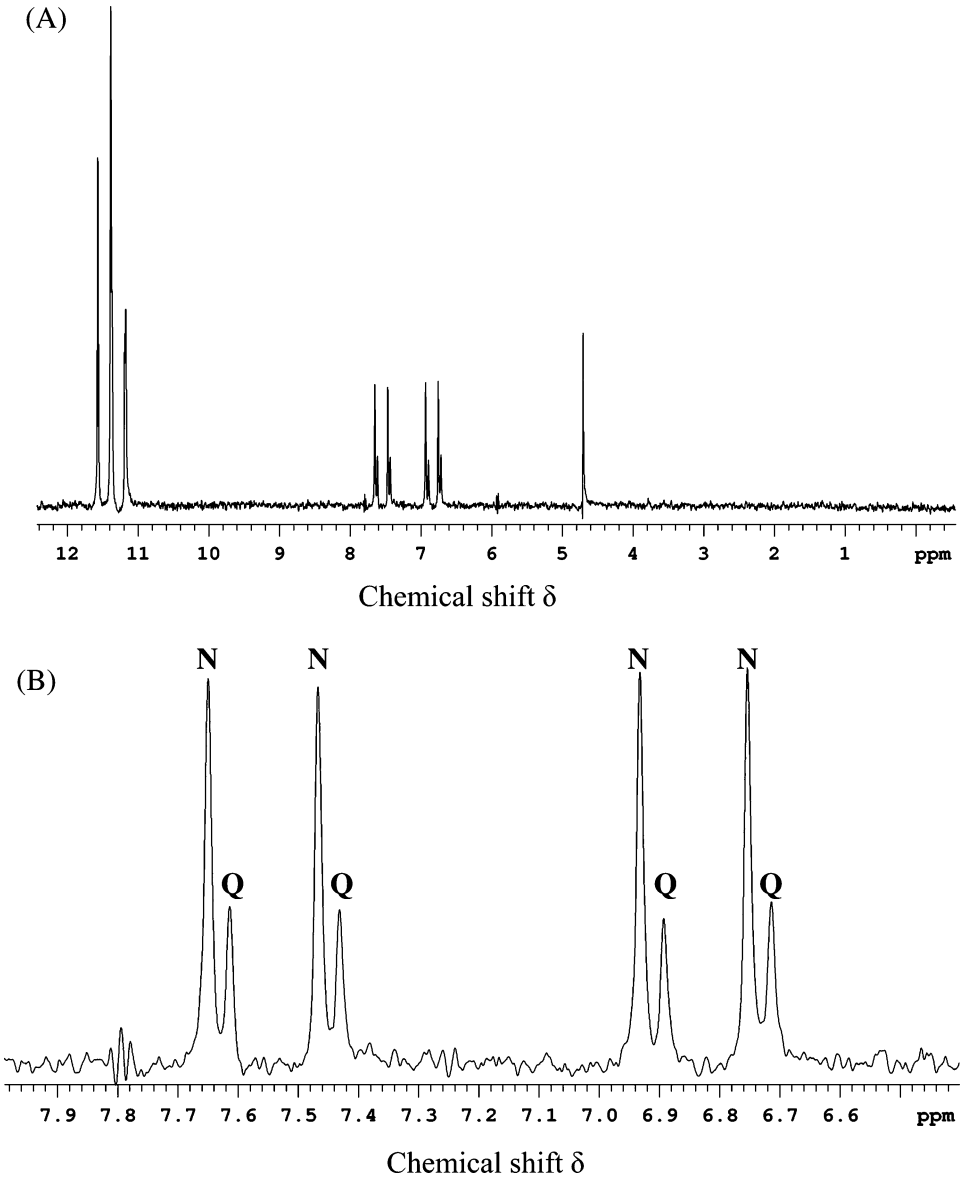

FIGURE 2: Isotope-edited (gHMQC) ^{1}H NMR spectrum. (A) Complete spectrum for a competition assay sample. (B) Expansion of the spectrum in the chemical shift region of 6.5−8.0 ppm showing the peaks from [^{15}N]Asn [labeled N; δ_{NHcis} 7.56 (d, J_{NH} = 90 Hz) and $\delta_{NHtrans}$ 6.84 (d, J_{NH} = 90 Hz)] and the additional peaks [labeled Q; δ_{NHcis} 7.52 (d, J_{NH} = 90 Hz) and $\delta_{NHtrans}$ 6.80 (d, J_{NH} = 90 Hz)] associated with incorporation of ^{15}N into the side chain amide of L-glutamine.

with aspartate and ATP in the presence of both glutamine (containing nitrogen isotopes at natural abundance) and $^{15}NH_4Cl$. In gHMQC spectra, resonances are observed for only hydrogen nuclei that (i) are attached to ^{15}N nuclei and (ii) are not in fast exchange. Hence, this NMR strategy permits a 30-fold increase in sensitivity over that for the direct acquisition of ^{15}N spectra. In addition, and very importantly for the goals of these experiments, the time needed to acquire ^{15}N-edited ^{1}H NMR spectra was approximately 3 orders of magnitude shorter than for the equivalent measurements using ^{15}N NMR spectroscopy. We were therefore able to obtain very "clean" ^{1}H NMR spectra for assay mixtures containing AS-B because the signals for protons on free $^{15}NH_3$ and $^{15}NH_4^+$ were not observed (Figure 2). Accurate integration of signals relative to those from an internal standard (uracil) was also possible, and standard curves relating the observed peak area of amide proton signals to the concentration of [^{15}N]asparagine present in solution under a variety of conditions were easily obtained (Figure 3). All of these results were carefully validated by independent measurements of asparagine using a HPLC-based assay (*40*).

Having established that the amount of [^{15}N]asparagine formed in the reaction could be quantitated using gHMQC spectroscopy, we studied whether the incorporation of ^{15}N from exogenous $^{15}NH_4Cl$ into asparagine could be suppressed by L-glutamine in the synthetase reaction catalyzed by AS-B. Thus, the recombinant bacterial enzyme was incubated with 100 mM $^{15}NH_4Cl$, saturating levels of MgATP, and aspartate at 10 and 20 mM in 100 mM HEPPS buffer (pH 8) over a range of L-glutamine concentrations (0−20 mM). Reactions were initiated by the addition of enzyme and allowed to proceed at 37 °C for 10 min before being quenched with TCA. Under these conditions, the final concentration of asparagine formed was 1−2 mM. This time was chosen so that the ^{15}N-labeled asparagine was formed in sufficiently high amounts for accurate quantitation using the HMQC-based assay. The reaction mixture was then separated into two portions, one of which was analyzed by

Table 1: AS-B-Catalyzed Incorporation of ^{15}N into L-Asparagine in the Steady State Competition Assays[a]

[Gln] (mM)	[$^{15}NH_4Cl$] (mM)	[[^{15}N]Gln] (mM)[b]	[[^{15}N]Asn] (mM)[b,c]	total Asn (mM)[d]	[^{14}N]Asn/[^{15}N]Asn
0	100	ND[e]	0.83 ± 0.03	0.83 ± 0.03	0
2.5	100	ND[e]	0.71 ± 0.02	1.22 ± 0.06	0.65 ± 0.08
10	100	0.18 ± 0.01	0.66 ± 0.02	1.30 ± 0.06	1.0 ± 0.1
20	100	0.26 ± 0.01	0.67 ± 0.01	1.4 ± 0.1	1.1 ± 0.2
40	100	0.34 ± 0.01	0.63 ± 0.03	1.4 ± 0.1	1.2 ± 0.2
20	0	ND[e]	ND[e]	0.76 ± 0.04	NA[f]
20	25	0.12 ± 0.01	0.29 ± 0.01	0.94 ± 0.03	2.2 ± 0.1
20	50	0.16 ± 0.02	0.44 ± 0.02	1.09 ± 0.05	1.5 ± 0.1
20	75	0.19 ± 0.01	0.62 ± 0.07	1.19 ± 0.07	1.1 ± 0.1
20	100	0.26 ± 0.01	0.67 ± 0.01	1.4 ± 0.1	1.1 ± 0.2

[a] All reaction mixtures contained 10 mM MgATP, 20 mM aspartate, 60 mM $MgCl_2$, and 490 nM AS-B in 100 mM HEPPS buffer (pH 8) (total volume of 2 mL). [b] As determined by gHMQC NMR spectroscopy. Errors are estimated on the basis of measurements employing known concentrations of authentic [^{15}N]Asn. [c] This value is corrected for the amount of [^{15}N]Asn that would be formed from [^{15}N]Gln at natural abundance, but the contribution of [^{14}N]Asn formed from any $^{14}NH_3$ released from the enzyme, as a result of the glutaminase activity of AS-B, is assumed to be negligible. [d] Mean value and standard deviation computed from two separate determinations on duplicate samples using reverse-phase HPLC. [e] Not detected. [f] Not applicable.

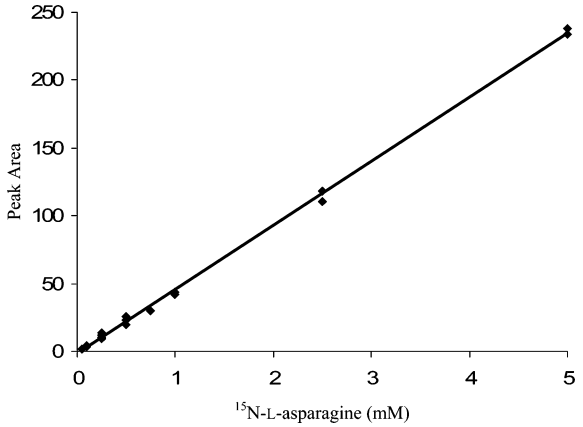

FIGURE 3: Standard curve relating the NMR peak area to the concentration of authentic [^{15}N]-L-asparagine. gHMQC ^1H spectra of [^{15}N]-L-asparagine (50, 100, 250, and 750 μM and 1, 2.5, and 5 mM) were recorded under the conditions of the competition assay in the absence of AS-B. Peak areas are expressed relative to those of the internal [^{15}N]uracil standard.

HPLC in determining the total amount of L-asparagine formed in the enzyme-catalyzed synthetase reaction. The second portion was transferred to a NMR tube, and the concentration of [^{15}N]asparagine formed under the assay conditions was determined using the gHMQC strategy. The dependence of incorporation of ^{15}N into the product amide on the initial concentration of L-glutamine was determined (Table 1), after correcting the amount of ^{15}N in L-asparagine to allow for the natural abundance of ^{15}N in L-glutamine. A similar set of experiments in which the concentration of L-glutamine was fixed at 20 mM and that of $^{15}NH_4Cl$ varied over a range of initial concentrations was also carried out (Table 1).

Somewhat unexpectedly, in light of the behavior reported for CPS in a similar competition experiment (*19*), we did not observe complete suppression of ^{15}N incorporation at saturating concentrations of L-glutamine [$K_{M(app)} = 0.69$ mM (*53*)]. Instead, the $^{14}N/^{15}N$ incorporation ratio exhibited saturation behavior, reaching a limiting value of 1.2 ± 0.2 as the concentration of L-glutamine was increased (Figure 4A). The ammonia dependence of the $^{14}N/^{15}N$ incorporation ratio when the initial concentration of L-glutamine was fixed at 20 mM was also examined and again showed substantial ^{15}N incorporation even at nonsaturating concentrations of $^{15}NH_3$ (Figure 4B). Any calculation of the expected $^{14}N/^{15}N$ ratio in the side chain of the product by the simple comparison of the *V*/*K* values for the two nitrogen sources is complicated, however, by the fact that L-asparagine inhibits the glutaminase activity of ASNS with an apparent K_I of 50−60 μM (*34*, *41*) while having no significant impact on the ammonia-dependent synthetase activity at 1 mM (*41*; also see the Supporting Information). Thus, the rate of ammonia-dependent L-asparagine synthesis is unaffected by the presence of L-asparagine over the period of our competition experiment, while that for glutamine-dependent synthetase activity decreases over time (Figure 4C). The effects of this differential inhibition are reflected in the total amount of L-asparagine formed after a given time under the assay conditions, which depends on whether one or both nitrogen sources are present. As a result, the total amount of L-asparagine formed in 10 min is greater when both exogenous ammonia and glutamine are present in solution than when glutamine is employed as the sole nitrogen source (Table 1). This also explains the observation that the total L-asparagine concentration is increased when ammonia is added to a solution containing a saturating amount (20 mM) of L-glutamine because ammonia-dependent activity is not inhibited by the binding of the reaction product to the glutaminase active site. Given this complication in understanding the apparent inability of L-glutamine to prevent incorporation of ^{15}N into asparagine, we sought to model the theoretical $^{14}N/^{15}N$ incorporation ratio as a function of either L-glutamine or ammonia concentration by kinetic simulations of the competition experiment (Scheme 2). In keeping with hypotheses developed from previous studies on CPS (*19*) and IGPS (*20*), we assumed that exogenous $^{15}NH_3$ and L-glutamine could not bind simultaneously to the E·ATP·Asp ternary complex required for synthetase activity (*40*, *41*). The assignment of rate constants was accomplished (*40*) on the basis of (i) direct NMR and HPLC measurements of the rate of L-asparagine production under the assay conditions (k_2, k_4, k_7, and k_{10}) and (ii) literature data on the steady state kinetics of AS-B (k_{-1}, k_{-3}, k_{-6}, and k_{-9}) (*40*, *53*). All second-order "on" rate constants were defined as 10^8 M^{-1} s^{-1}, although this does not account for conformational changes that might take place on substrate binding. Perhaps more importantly, we assumed that (i) the presence of L-asparagine in the glutaminase active site of the enzyme does not affect rate constants associated with ammonia-

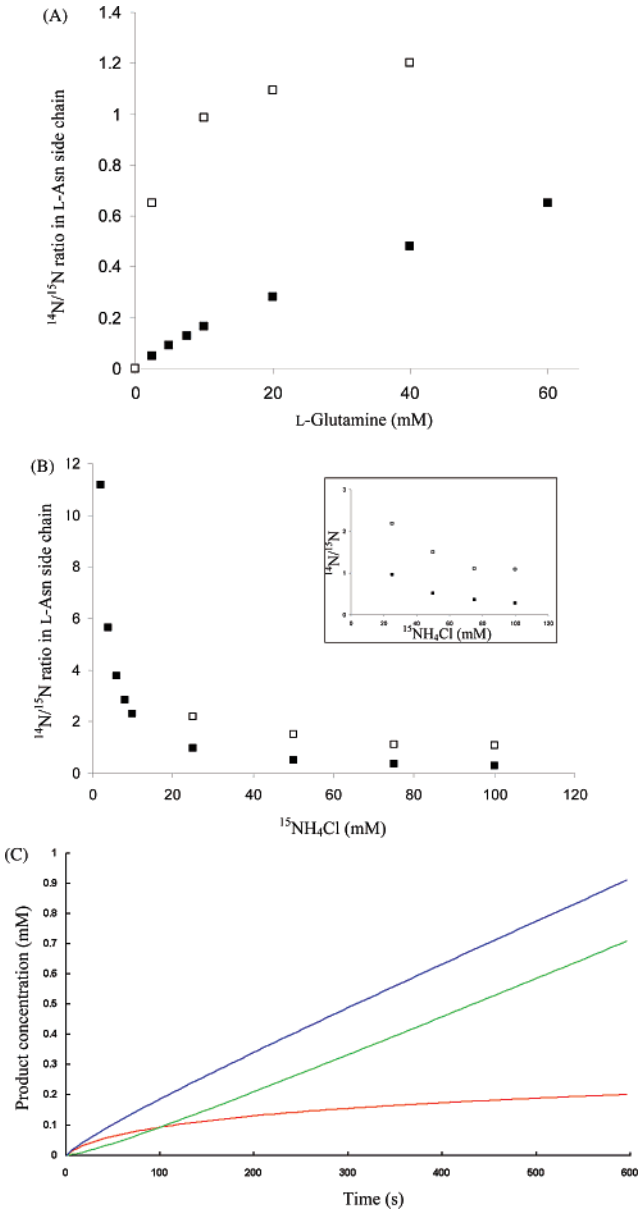

FIGURE 4: $^{14}N/^{15}N$ incorporation ratios in L-asparagine formed by the AS-B synthetase reaction under competition assay conditions. (A) Comparison of the experimentally observed (□) and simulated (■) $^{14}N/^{15}N$ incorporation ratio in 100 mM HEPPS buffer (pH 8) containing 10 mM MgATP, 20 mM aspartate, and 100 mM $^{15}NH_4Cl$. (B) Comparison of the experimentally observed (□) and simulated (■) $^{14}N/^{15}N$ incorporation ratio in 100 mM HEPPS buffer (pH 8) containing 10 mM MgATP, 20 mM aspartate, and 20 mM L-glutamine. The inset shows an expanded view of the plot for the experimental $^{14}N/^{15}N$ ratios. (C) Kinetic simulation of the time-dependent formation of total L-asparagine (blue), [^{14}N]-L-asparagine (red), and [^{15}N]-L-asparagine (green) showing the impact of differential inhibition of the two synthetase reactions by L-asparagine.

dependent synthetase activity (k_4, k_7, and k_{10}) and (ii) the "off" rate for asparagine leaving the inhibitory site is not affected by bound ammonia (k_{-11} and k_{-12}). The only remaining unknown rate constants (k_{-11} and k_{-12}) in this simple model could then be estimated from the observed K_I for L-asparagine in the glutamine-dependent synthetase reaction. Although this kinetic model exhibits a time-dependent decrease in the rate of incorporation of nitrogen from L-glutamine to give [^{14}N]-L-asparagine in the competition assay (Figure 4C), it does not qualitatively reproduce the saturation behavior of the $^{14}N/^{15}N$ incorporation ratio as the concentration of L-glutamine is increased in the presence of a fixed amount of $^{15}NH_4Cl$ (Figure 4A). The lack of quantitative agreement between the experimental and simulated $^{14}N/^{15}N$ incorporation ratios likely arises from an overestimation of the affinity of the AS-B glutaminase domain for L-asparagine, and we therefore conclude that both nitrogen sources can be present on the enzyme simultaneously.

^{15}N Exchange Experiments. Evidence to support (i) the conclusion from the kinetic simulations and (ii) the hypothesis that $^{15}NH_3$ might be able to access the N-terminal glutaminase site (and presumably the intramolecular tunnel) when L-glutamine is also present came from the observation of peaks in the isotope-edited gHMQC spectrum with chemical shift values that were different from those of the resonances arising from the amide protons of [^{15}N]asparagine (Figure 2B). The acquisition of ^1H spectra for the reaction mixture in the absence of isotopic editing, but with suppression of the water signal, showed that these unexpected peaks were satellites of the broad signal from the amide protons in [^{14}N]-L-glutamine (Figure 5). As a result, we concluded that these signals arose from amide protons bonded to ^{15}N in the side chain of L-glutamine. Control experiments established that $^{14}N-^{15}N$ exchange did not occur in the absence of AS-B, so this reaction was examined in more detail by incubating the enzyme with $^{15}NH_4Cl$ in the presence of glutamine and ATP. Under these conditions, the rate of ^{15}N-substituted glutamine formation (i) showed saturation behavior with respect to glutamine at a fixed concentration (100 mM) of $^{15}NH_4Cl$ (Figure 6) and (ii) was linearly dependent on the concentration of exogenous $^{15}NH_4Cl$ (data not shown). A kinetic model was constructed to describe the $^{14}N-^{15}N$ exchange (Figure 7A), which gave the following equation for partitioning of the thioester intermediate at the steady state to yield [^{15}N]-L-glutamine (see the Supporting Information):

$$v = \frac{k_1 k_2 [E]_T [Gln][^{15}NH_4^+]}{k_1[Gln] + k_2[^{15}NH_4^+] + k_3[H_2O]} \quad (1)$$

where v is the rate of [^{15}N]glutamine production via the exchange reaction in the presence of ATP but in the absence of aspartate and k_1, k_2, and k_3 are microscopic rate constants with estimated values of 5.1, 7.8×10^{-3}, and 1.06×10^{-4} mM^{-1} s^{-1}, respectively, assuming that hydrolysis of the thioester intermediate is the rate-limiting step in the glutaminase reaction (*43*). Using these values in our model for the exchange reaction gave excellent agreement between the observed concentrations of [^{15}N]glutamine and those expected from kinetic simulation at a variety of NH_4Cl concentrations (Figure 7B). Having established a firm understanding of this reaction in the absence of aspartate, we next examined whether the overall rate of $^{14}N-^{15}N$ exchange was altered when AS-B was undergoing catalytic turnover to yield asparagine. An analysis similar to that described above showed that our kinetic model gave excellent agreement with experimental values (data not shown) when the microscopic rate constants k_1, k_2, and k_3 were assigned values of 9.6, 1.8×10^{-2}, and 8.8×10^{-5} mM^{-1} s^{-1}, respectively. The similarity of these rate constants to those

Scheme 2: Kinetic Model for the Competition between $^{15}NH_3$ and [^{14}N]Gln in the AS-B Synthetase Reaction[a]

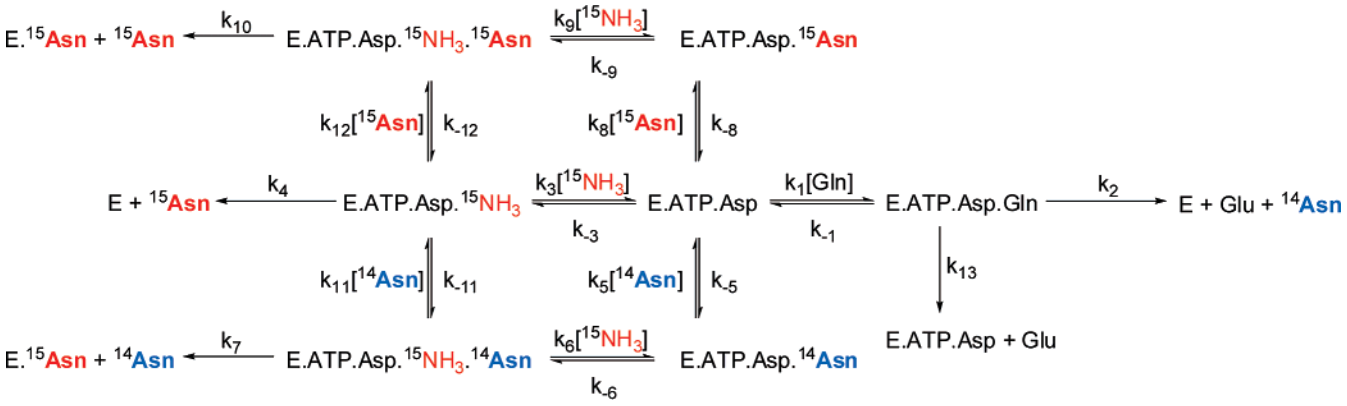

[a] Note the key assumptions that (i) $^{15}NH_3$ and L-glutamine cannot both be present on the enzyme simultaneously, (ii) L-asparagine is a competitive inhibitor of the glutamine-dependent synthetase activity (*41*), and (iii) the concentration of $^{14}NH_3$ in bulk solution is not sufficiently high for this species to be employed in asparagine synthesis after it leaves the enzyme. Kinetic simulations of this model employed the following values for the microscopic rate constants (see the text for details): $k_1 = k_3 = k_5 = k_6 = k_8 = k_9 = k_{11} = k_{12} = 10^8$ M^{-1} s^{-1}, $k_{-1} = 6.9 \times 10^4$ s^{-1}, $k_2 = 6.36$ s^{-1}, $k_{-3} = k_{-6} = k_{-9} = 1.7 \times 10^6$ s^{-1}, $k_4 = k_7 = k_{10} = 3.19$ s^{-1}, $k_{-5} = k_{-8} = k_{-11} = k_{-12} = 8.7 \times 10^2$ s^{-1}, and $k_{13} = 5.09$ s^{-1}.

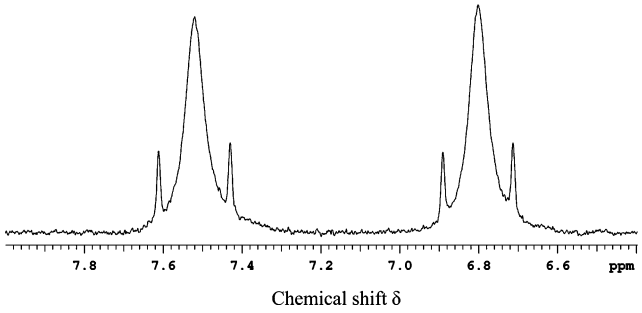

FIGURE 5: Unedited ^{1}H NMR spectrum of the exchange reaction assay mixture. The two broad peaks arise from the two nonequivalent protons coupled to ^{14}N in the amide of L-glutamine, while the satellite peaks are for the cognate protons in [^{15}N]Gln.

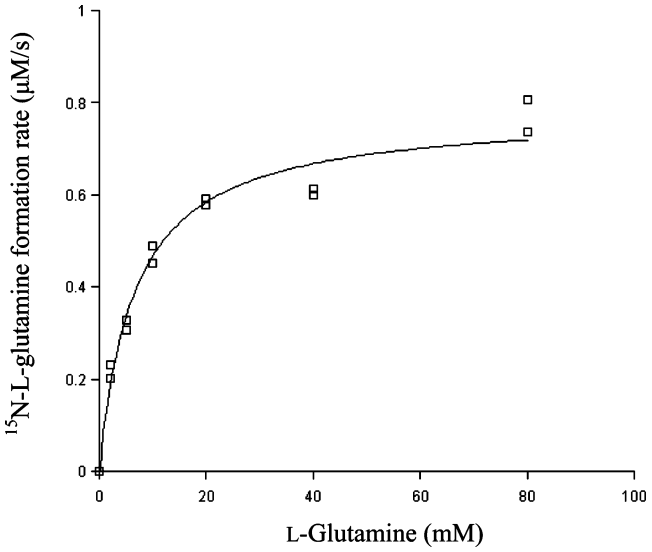

FIGURE 6: Glutamine dependence of the exchange of $^{15}NH_3$ into L-glutamine under exchange assay conditions. Exchange reactions were performed in 100 mM HEPPS buffer (pH 8) containing 60 mM $MgCl_2$, 10 mM ATP, and 100 mM $^{15}NH_4Cl$ (total volume of 2 mL), and each data point represents an average of duplicate experiments.

determined for ^{14}N−^{15}N exchange in the absence of aspartate suggests that the molecular mechanism of the reaction is identical under both sets of conditions.

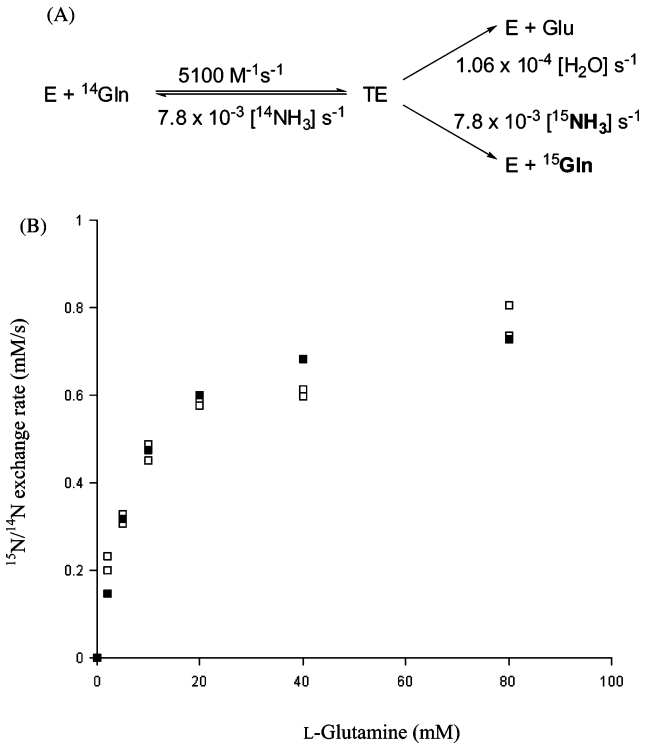

FIGURE 7: Exchange of $^{15}NH_3$ into L-glutamine during the glutaminase reaction catalyzed by AS-B. (A) Kinetic model employed in the simulations of this exchange process. (B) Comparison of the experimentally observed (□) and simulated (■) rate of exchange of $^{15}NH_3$ into L-glutamine when AS-B is incubated in 100 mM HEPPS buffer (pH 8) with L-glutamine and 100 mM $^{15}NH_4Cl$ in the absence of ATP and aspartate.

The simplest explanation for ^{14}N−^{15}N exchange is that ^{15}N-substituted glutamine is formed by reaction of exogenous $^{15}NH_3$ with a thioester intermediate formed in the N-terminal active site during the enzyme-catalyzed hydrolysis of glutamine (Scheme 3) (*43*, *54*). This is an intriguing finding because a similar ^{14}N−^{15}N exchange reaction involving the side chain amide of L-glutamine was not observed in similar competition experiments employing CPS (*19*), although it is possible that the amounts of ^{15}N-substituted glutamine that formed might have been too small for detection by ^{15}N NMR spectroscopy. In addition, this phenomenon has not been described previ-

Scheme 3: Hypothetical Mechanism for Formation of a Thioester Intermediate during the ASNS-Catalyzed Hydrolysis of L-Glutamine[a]

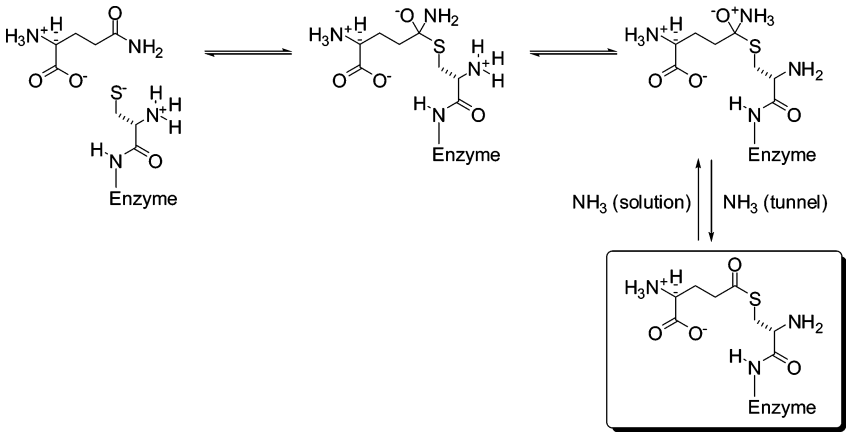

[a] Note that the N-terminal amino group is thought to function as the general acid/base in the reaction (*17*, *55*), although direct evidence for this proposal remains to be obtained in the case of ASNS. The thioester intermediate (TE), which subsequently reacts with water to give glutamate, is drawn within a box.

ously, to the best of our knowledge, for any other glutamine-dependent amidotransferase. The molecular pathway by which $^{15}NH_3$ gains access to the N-terminal, glutaminase site remains to be determined. Hence, it is possible that exogenous ammonia can access the N-terminal domain directly as a consequence of the enzyme adopting a conformation in which the tunnel linking the two active sites is solvent accessible. Alternatively, ammonia might enter the intramolecular tunnel linking the two active sites after entering the C-terminal domain. In both mechanisms, ammonia could displace water molecules in the tunnel prior to glutamine binding and the adoption of the "closed" conformation observed in the crystal structure of the enzyme.

CONCLUSIONS

In summary, we have reported a sensitive, quantitative, and reproducible isotope-edited ^1H NMR assay for monitoring the incorporation of ^{15}N into the side chain amide of L-asparagine. Spectra can be obtained rapidly, thereby permitting the examination of a wide variety of conditions for these steady state competition experiments. The application of this assay to the reaction catalyzed by AS-B has shown, somewhat unexpectedly, that high concentrations of glutamine cannot suppress the incorporation of ^{15}N from exogenous $^{15}NH_3$. This result, in combination with our observation that exogenous ammonia can trap the thioester intermediate in the glutaminase reaction, is consistent with a model in which the putative ammonia channel linking the N- and C-terminal active sites can be accessed by $^{15}NH_3$ molecules at some point during catalytic turnover. This behavior seems to contrast with previous findings concerning ammonia channeling in class I amidotransferases, such as CPS (*19*) and IGPS (*20*), which appear to have been optimized during evolution for (i) high nitrogen transfer efficiency (*19*) and (ii) tight kinetic coupling of glutaminase and synthetase activities (*20*, *23*). In part, this may be a consequence of the ability of asparagine to inhibit nonproductive glutaminase activity, which might have relaxed any evolutionary pressure to construct intradomain interactions needed for efficient kinetic coupling of catalysis in the two active sites of asparagine synthetase.

Any interpretation of the inability of saturating glutamine to suppress ammonia-dependent synthetase activity in terms of molecular structure is complicated by the observed solvent inaccessibility of the intramolecular tunnel that is observed in the high-resolution crystal structure of AS-B (*12*). We have shown previously, however, that coupling of the glutaminase and synthetase activities of the enzyme appears to break down as the glutamine concentration is increased (*40*), perhaps because of a conformational change that permits the release of ammonia ($^{14}NH_3$) from one or both of the glutaminase sites. It is therefore possible that molecules of exogenous ammonia ($^{15}NH_3$) might be able to gain access to the synthetase site when the enzyme adopts this conformation, the result being that high concentrations of L-glutamine fail to suppress ^{15}N incorporation to the extent seen for other amidotransferases.

ACKNOWLEDGMENT

We thank Robert Harker (University of Florida) for useful discussions regarding many technical aspects of the gHMQC NMR measurements.

SUPPORTING INFORMATION AVAILABLE

Effect of asparagine on the ammonia-dependent synthetase activity of AS-B and modeling AS-B-catalyzed the exchange of ^{15}N from $^{15}NH_4Cl$ to L-glutamine. This material is available free of charge via the Internet at http://pubs.acs.org.

REFERENCES

1. Zalkin, H., and Smith, J. L. (1998) Enzymes using glutamine as an amide donor, *Adv. Enzymol. Relat. Areas Mol. Biol. 72*, 87−144.
2. Zalkin, H. (1993) The amidotransferases, *Adv. Enzymol. Relat. Areas Mol. Biol. 66*, 203−309.
3. Buchanan, J. M. (1973) The amidotransferases, *Adv. Enzymol. Relat. Areas Mol. Biol. 39*, 91−183.
4. Oshikane, H., Sheppard, K., Fukai, S., Nakamura, Y., Ishitani, R., Numata, T., Sherrer, R. L., Feng, L., Schmitt, E., Panvert, M., Blanquet, S., Mechulam, Y., Söll, D., and Nureki, O. (2006) Structural basis of RNA-dependent recruitment of glutamine to the genetic code, *Science 312*, 1950−1954.
5. Nakamura, A., Yao, M., Chimnaronk, S., Sakai, N., and Tanaka, I. (2006) Ammonia channel couples glutaminase with transamidase reactions in GatCAB, *Science 312*, 1954−1958.
6. Mouilleron, S., Badet-Denisot, M.-A., and Golinelli-Pimpaneau, B. (2006) Glutamine binding opens the ammonia channel and activates glucosamine-6P synthase, *J. Biol. Chem. 281*, 4404−4412.

7. Anand, R., Hoskins, A. A., Stubbe, J., and Ealick, S. E. (2004) Domain organization of *Salmonella typhimurium* formylglycinamide ribonucleotide amidotransferases revealed by X-ray crystallography, *Biochemistry 43*, 10328−10342.
8. Endrizzi, J. A., Kim, H., Anderson, P. M., and Baldwin, E. P. (2004) Crystal structure of *Escherichia coli* cytidine triphosphate synthetase, a nucleotide-regulated glutamine amidotransferases/ATP-dependent amidoligase fusion protein and homologue of anticancer and antiparasitic drug targets, *Biochemistry 43*, 6447−6463.
9. Myers, R. S., Jensen, J. R., Deras, I. L., Smith, J. L., and Davisson, V. J. (2003) Substrate-induced changes in the ammonia channel for imidazole glycerol phosphate synthase, *Biochemistry 42*, 7003−7012.
10. van den Heuvel, R. H. H., Ferrari, D., Bossi, R. T., Ravasio, S., Curti, B., Vanoni, M. A., Florencio, F. J., and Mattevi, A. (2002) Structural studies on the synchronization of catalytic centers in glutamate synthase, *J. Biol. Chem. 277*, 24579−24583.
11. Douangamath, A., Walker, M., Beismann-Driemeyer, S., Vega-Fernandez, M. C., Sterner, R., and Wilmanns, M. (2002) Structural evidence for ammonia tunneling across the $(\beta\alpha)_8$ barrel of the imidazole glycerol phosphate synthase bienzyme complex, *Structure 10*, 185−193.
12. Larsen, T. M., Boehlein, S. K., Schuster, S. M., Richards, N. G. J., Thoden, J. B., Holden, H. M., and Rayment, I. (1999) The three-dimensional structure of *Escherichia coli* asparagine synthetase B. A short journey from substrate to product, *Biochemistry 38*, 16146−16157.
13. Huang, X., Holden, H. M., and Raushel, F. (2001) Channeling of substrates and intermediates in enzyme-catalyzed reactions, *Annu. Rev. Biochem. 70*, 149−180.
14. Raushel, F. M., Thoden, J. B., and Holden, H. M. (1999) The amidotransferase family of enzymes: Molecular machines for the production and delivery of ammonia, *Biochemistry 38*, 7891−7899.
15. Richards, N. G. J., and Kilberg, M. S. (2006) Asparagine synthetase chemotherapy, *Annu. Rev. Biochem. 75*, 629−654.
16. Binda, C., Bossi, R. T., Wakatsuki, S., Arzt, S., Coda, A., Curti, B., Vanoni, M. A., and Mattevi, A. (2000) Cross-talk and ammonia channeling between active centers in the unexpected domain arrangement of glutamate synthase, *Structure 8*, 1299−1308.
17. Massière, F., and Badet-Denisot, M.-A. (1998) The mechanism of glutamine-dependent amidotransferases, *Cell. Mol. Life Sci. 54*, 205−222.
18. Weeks, A., Lund, L., and Raushel, F. M. (2006) Tunneling of intermediates in enzyme-catalyzed reactions, *Curr. Opin. Chem. Biol. 10*, 465−472.
19. Mullins, L. S., and Raushel, F. M. (1999) Channeling of ammonia through the intermolecular tunnel contained within carbamoyl phosphate synthetase, *J. Am. Chem. Soc. 121*, 3803−3804.
20. Myers, R. S., Amaro, R. E., Luthey-Schulten, Z. A., and Davisson, V. J. (2005) Reaction coupling through interdomain contacts in imidazole glycerol phosphate synthase, *Biochemistry 44*, 11974−11985.
21. Willemoës, M. (2004) Competition between ammonia derived from internal glutamine hydrolysis and hydroxylamine present in the solution for incorporation into UTP as catalysed by *Lactococcus lactis* CTP synthase, *Arch. Biochem. Biophys. 424*, 105−111.
22. Bera, A. K., Smith, J. L., and Zalkin, H. (2000) Dual role for the glutamine phosphoribosylpyrophosphate amidotransferase ammonia channel: Interdomain signaling and intermediate channeling, *J. Biol. Chem. 275*, 7975−7979.
23. Miles, B. W., and Raushel, F. M. (2000) Synchronization of the three reaction centers within carbamoyl phosphate synthetase, *Biochemistry 39*, 5051−5056.
24. Kim, J., and Raushel, F. M. (2004) Perforation of the tunnel wall in carbamoyl phosphate synthetase derails the passage of ammonia between sequential active sites, *Biochemistry 43*, 5334−5340.
25. Thoden, J. B., Huang, X., Raushel, F. M., and Holden, H. M. (2002) Carbamoyl phosphate synthetase: Creation of an escape route for ammonia, *J. Biol. Chem. 277*, 39722−39727.
26. Chaudhuri, B. N., Lange, S. C., Myers, R. S., Davisson, V. J., and Smith, J. L. (2003) Toward understanding the mechanism of the complex cyclization reaction catalyzed by imidazole glycerolphosphate synthase: Crystal structures of a ternary complex and the free enzyme, *Biochemistry 42*, 7003−7012.
27. Amaro, R. E., Myers, R. S., Davisson, V. J., and Luthey-Schulten, Z. A. (2005) Structural elements in IGP synthase exclude water to optimize ammonia transfer, *Biophys. J. 89*, 475−487.
28. Luthey-Schulten, Z. A., and Amaro, R. (2004) Molecular dynamics simulations of substrate channeling through an α/β barrel protein, *Chem. Phys. 307*, 147−155.
29. Amaro, R., Tajkhorshid, E., and Luthey-Schulten, Z. (2003) Developing an energy landscape for the novel function of a $(\beta/\alpha)_8$ barrel: Ammonia conduction through HisF, *Proc. Natl. Acad. Sci. U.S.A. 100*, 7599−7604.
30. Smith, J. L. (1995) Structures of glutamine amidotransferases from the purine biosynthetic pathway, *Biochem. Soc. Trans. 23*, 894−898.
31. Brannigan, J. A., Dodson, G., Duggleby, H. J., Moody, P. C. E., Smith, J. L., Tomchick, D. R., and Murzin, A. G. (1995) A protein catalytic framework with an N-terminal nucleophile is capable of self-activation, *Nature 378*, 416−419.
32. Bieganowski, P., Pace, H. C., and Brenner, C. (2003) Eukaryotic NAD^+ synthetase Qns1 contains an essential, obligate intramolecular thiol glutaminase domain related to nitrilase, *J. Biol. Chem. 278*, 33049−33055.
33. Richards, N. G. J., and Schuster, S. M. (1998) Mechanistic issues in asparagine synthetase catalysis, *Adv. Enzymol. Relat. Areas Mol. Biol. 72*, 145−198.
34. Sheng, S., Moraga-Amador, D. A., Van Heeke, G., Allison, R. D., Richards, N. G. J., and Schuster, S. M. (1993) Glutamine inhibits the ammonia-dependent activities of two Cys-1 mutants of human asparagine synthetase through the formation of an abortive complex, *J. Biol. Chem. 268*, 16771−16780.
35. Fresquet, V., Thoden, J. B., Holden, H. M., and Raushel, F. M. (2004) Kinetic mechanism of asparagine synthetase from *Vibrio cholerae*, *Bioorg. Chem. 32*, 63−75.
36. Badet, B., Vermoote, P., Haumont, P. Y., Lederer, F., and LeGoffic, F. (1987) Glucosamine synthetase from *Escherichia coli*: Purification, properties and glutamine-utilizing site location, *Biochemistry 26*, 1940−1948.
37. Kim, J. H., Krahn, J. M., Tomchick, D. R., Smith, J. L., and Zalkin, H. (1996) Structure and function of the glutamine phosphoribosylpyrophosphate amidotransferase glutamine site and communication with the phosphoribosylpyrophosphate site, *J. Biol. Chem. 271*, 15549−15557.
38. Vanoni, M. A., and Curti, B. (2004) Glutamate synthase: A fascinating pathway from glutamine to glutamate, *Mol. Life Sci. 61*, 669−681.
39. Ciustea, M., Gutierrez, J. A., Abbatiello, S. E., Eyler, J. R., and Richards, N. G. J. (2005) Efficient expression, purification and characterization of C-terminally tagged, recombinant human asparagine synthetase, *Arch. Biochem. Biophys. 440*, 18−27.
40. Tesson, A. R., Soper, T. S., Ciustea, M., and Richards, N. G. J. (2003) Revisiting the steady state kinetic mechanism of glutamine-dependent asparagine synthetase from *Escherichia coli*, *Arch. Biochem. Biophys. 413*, 23−31.
41. Boehlein, S. K., Stewart, J. D., Walworth, E. S., Thirumoorthy, R., Richards, N. G. J., and Schuster, S. M. (1998) Kinetic mechanism of *Escherichia coli* asparagine synthetase B, *Biochemistry 37*, 13230−13238.
42. Hurd, R. E., and John, B. K. (1991) Gradient-enhanced proton-detected heteronuclear multiple-quantum coherence spectroscopy, *J. Magn. Reson. 91*, 648−653.
43. Schnizer, H., Boehlein, S. K., Stewart, J. D., Richards, N. G. J., and Schuster, S. M. (1999) Formation and isolation of a covalent intermediate during the glutaminase reaction of a Class II amidotransferases, *Biochemistry 38*, 3677−3682.
44. Boehlein, S. K., Richards, N. G. J., and Schuster, S. M. (1994) Glutamine-dependent nitrogen transfer in *Escherichia coli* asparagine synthetase B: Searching for the catalytic triad, *J. Biol. Chem. 269*, 7450−7457.
45. Bradford, M. M. (1976) Rapid and sensitive method for quantitation of microgram quantities of protein utilizing principle of protein-dye binding, *Anal. Biochem. 72*, 248−254.
46. Thompson, J. S., and Edmonds, O. P. (1980) Safety aspects of handling the potent allergen FDNB, *Ann. Occup. Hyg. 23*, 27−33.
47. Mendes, P. (1993) GEPASI: A software package for modeling the dynamics, steady states and control of biochemical and other systems, *Comput. Appl. Biosci. 9*, 563−571.
48. Mendes, P. (1997) Biochemistry by the numbers: Simulation of biochemical pathways with GEPASI 3, *Trends Biochem. Sci. 22*, 361−363.
49. Willmöes, M. (2004) Competition between ammonia derived from internal glutamine hydrolysis and hydroxylamine present in the

solution for incorporation into UTP as catalysed by *Lactococcus lactis* CTP synthase, *Arch. Biochem. Biophys. 424*, 105−111.
50. Bearne, S. L., Hekmat, O., and MacDonnell, J. E. (2001) Inhibition of *Escherichia coli* CTP synthase by glutamine γ-semialdehyde and the role of the allosteric effector GTP in glutamine hydrolysis, *Biochem. J. 356*, 223−232.
51. Levitzki, A., and Koshland, D. E., Jr. (1971) Cytidine triphosphate synthetase. Covalent intermediates and mechanism of action, *Biochemistry 10*, 3365−3371.
52. Zalkin, H., and Truitt, C. D. (1977) Characterization of the glutamine site of *Escherichia coli* guanosine 5′-monophosphate synthetase, *J. Biol. Chem. 252*, 5431−5436.
53. Boehlein, S. K., Schuster, S. M., and Richards, N. G. J. (1996) Probing nitrogen transfer using glutamic acid γ-monohydroxamate and hydroxylamine as alternate substrates for *Escherichia coli* asparagine synthetase B, *Biochemistry 35*, 3031−3037.
54. Schnizer, H. G., Boehlein, S. K., Stewart, J. D., Richards, N. G. J., and Schuster, S. M. (2002) γ-Glutamyl thioester intermediate in the glutaminase reaction catalyzed by *Escherichia coli* asparagine synthetase B, *Methods Enzymol. 354*, 260−271.
55. Peräkylä, M., and Kollman, P. A. (1997) A simulation of the catalytic mechanism of aspartylglucosaminidase using *ab initio* quantum mechanics and molecular dynamics, *J. Am. Chem. Soc. 119*, 1189−1196.
56. Humphrey, W., Dalke, A., and Schulten, K. (1996) VMD: Visual molecular dynamics, *J. Mol. Graphics 14*, 33−38.

BI700145T